Tan, M., McInnes, C. and Ceriotti, M. (2018) Capture of small near-Earth asteroids to Earth orbit using aerobraking. *Acta Astronautica*, 152, pp. 185-195. (doi:10.1016/j.actaastro.2018.08.007)

Capture of small near-Earth asteroids to Earth orbit using aerobraking

Minghu Tan*, Colin McInnes, Matteo Ceriotti

School of Engineering, University of Glasgow, Glasgow G12 8QQ, UK

Abstract

This paper investigates the concept of capturing near-Earth asteroids into bound orbits around the Earth by using aerobraking. To guarantee that the candidate asteroids cannot present an impact risk during aerobraking, an initial aerobraking hazard analysis is undertaken and accordingly only asteroids with a diameter less than 30 m are considered as candidates in this paper. Then, two asteroid capture strategies utilizing aerobraking are defined. These are termed single-impulse capture and bi-impulse capture, corresponding to two approaches to raising the perigee height of the captured asteroid's orbit after the aerobraking manoeuvre. A Lambert arc in the Sun-asteroid two-body problem is used as an initial estimate for the transfer trajectory to the Earth and then a global optimisation is undertaken, using the total transfer energy cost and the retrieved asteroid mass ratio (due to ablation) as objective functions. It is shown that the aerobraking can in principle enable candidate asteroids to be captured around the Earth with, in some cases, extremely low energy requirements.

Keywords: Circular restricted three-body problem; asteroid capture; aerobraking; Earth; low energy

* Corresponding author.

E-mail address: m.tan.2@research.gla.ac.uk (Minghu Tan).

1. Introduction

Many authors have noted that asteroids can provide key information on the formation and evolution of the solar system, and thus a series of asteroid exploration missions have been undertaken or are planned [1-4]. Among the family of asteroids, near-Earth asteroids have gained significant attention due to their accessibility. Moreover, near-Earth asteroids are also considered to provide useful resources which can be used to support future space activities, such as in-situ spacecraft propellant manufacturing and life support consumables [5]. Therefore, the exploitation and utilisation of these resources has generated a growing interest in low-energy strategies to capture near-Earth asteroids into the vicinity of the Earth [6-8]. One of the main challenges for asteroid capture missions is the limitation on retrieval mass with current propulsion technologies. Hence, reducing the total energy cost of capturing near Earth asteroids is key to future asteroid capture missions and will be the focus of this paper.

Most recent research work has investigated the possibility of capturing near-Earth asteroids in the vicinity of the Earth, including the Sun-Earth libration points L_1 and L_2 [9-12], the neighbourhood of the Moon [13-15] and bound orbits about the Earth itself [8, 16, 17]. As vantage points for space observatories, and candidate gateways for future deep space exploration, the Sun-Earth L_1 and L_2 points also serve as the ideal locations for captured asteroids due to their unique locations and dynamical characteristics [18]. In prior papers, the stable manifolds associated with the Sun-Earth L_1 and L_2 points were employed to design transfer trajectories to enable the capture of near Earth asteroids [9, 19, 20]. The utilisation of stable manifolds is also the key to achieving low-cost capture, since flight along the stable manifold is ballistic and no deterministic manoeuvre is required during this period. Based on these characteristics, a family of Easily Retrievable Objects (EROs) with a total capture cost of less than 500m/s can be found by patching the Lambert problem in the Sun-centred two-body problem and the stable manifolds of the L_1 and L_2 points in the Sun-Earth circular restricted three-body problem [9]. Moreover, to increase the number of potentially easily retrievable objects [12], low thrust propulsion has been employed to design the transfer between the asteroid's initial orbit and the appropriate stable manifold [10, 12]. Meanwhile, other families of final periodic orbits (distant retrograde orbits) around the Sun-Earth L_1 and L_2 points have also been investigated for capture [11].

Moreover, momentum exchange theory has been used to attempt to lower the total cost of capturing asteroids at the Sun-Earth L_1 and L_2 points, including engineered impacts between asteroids and tethered assists [21]. The neighbourhood of the Moon has also been viewed as a preferred location for captured asteroids. NASA proposed a near-Earth asteroid redirect mission (ARM) to capture an asteroid (or portion of an asteroid) into a distant retrograde orbit around the Moon [13]. Based on the results of capturing asteroids around the Sun-Earth L_1 and L_2 points, the idea of capturing asteroids around the Earth-Moon L_2 point has also been investigated by patching stable manifolds in the Earth-Moon system and unstable manifolds in the Sun-Earth system [14]. To save flight time, a direct asteroid capture strategy was also defined by designing a direct transfer between the candidate asteroid's orbit and the appropriate stable manifold associated with the Earth-Moon L_2 point using differential corrections [15]. Furthermore, there exists two types of asteroid capture strategies around the Earth, corresponding to two different dynamical models. The first is to directly capture an asteroid into an elliptic orbit around the Earth with the transfer trajectory designed by patching together the Sun-Earth circular restricted three-body problem and Earth-centred two-body problem [8]. In the other strategy, the motion of the captured asteroid is always modelled as a multi-body problem and the Kolmogorov–Arnold–Moser (KAM) method can be used to capture an asteroid temporarily in the Earth's Hill regions [17] (although the capture duration is extremely long for practical purposes). Moreover, to reduce the total capture cost, a lunar flyby can also be used in this multi-body environment [16].

On a grazing approach to a planetary body, the planet's atmosphere may provide an aerobraking manoeuvre and thereby directly reduce the speed of the object through energy dissipation. Recently, technologies for such aerobraking manoeuvres have been studied extensively [22-25], with the Magellan [26] and MGS [27] spacecraft demonstrating the feasibility of multi-pass aerobraking for robotic missions. Moreover, Earth aerobraking has been also been proposed to design Earth-return trajectories from Mars [28] or to transfer to a low Earth orbit from a generic hyperbolic trajectory [29]. Moreover, Sonter [5] proposed the use of an "Earth-fabricated, LEO-fabricated, or asteroid-fabricated aerobrake" to return captured asteroid material to low Earth orbit. Manufacturing an engineered aerobrake directly from asteroid material offers interesting possibilities for the future. Baoyin, Chen and Li [30] supposed that aerobraking would greatly reduce the velocity increment required to capture an asteroid into a bound orbit around the Earth. Based on a first order approximation of the aerobraking manoeuvre [31], Sanchez and McInnes [32] investigated the relationship between the mass loss of the captured asteroid due to ablation and the required compressive strength of the asteroid material during aerobraking. They then estimated the number of 10 m diameter asteroids which could in principle be captured by using an aerobraking strategy. In addition, the utilisation of Earth aerobraking was proposed to deliver a captured asteroid with a diameter of less than 2 m to the International Space Station as a proof-of-concept mission [33].

In our previous work, we proposed to combine an Earth gravity assist and a small aerobraking manoeuvre with invariant manifolds to capture an asteroid into a periodic orbit around the Sun-Earth libration points L_1 and L_2 [34]. This paper will provide a much more general analysis of aerobraking strategies and will use aerobraking to capture asteroids directly into bound orbits around the Earth. A key issue for capturing asteroids using Earth aerobraking is clearly the potential for impact of the captured asteroid during a grazing flyby of the Earth in the event of manoeuvre errors. To address this problem, only small near-Earth asteroids which in principle would ablate completely before reaching the Earth's surface, and so would not represent a risk, will be considered in this paper. Clearly, an accurate and robust navigation and control strategy would also be required. The use of an engineered aerobrake manufactured from asteroid material also offers advantages for more precise aerocapture, and greater mass returned, rather than directly ablating the surface of the asteroid itself during the manoeuvre [35].

In this paper, models of the circular restricted three-body problem and the aerobraking manoeuvre are firstly introduced and then the height threshold for aerobraking above the Earth's surface is determined. According to a preliminary asteroid risk analysis, small asteroids with a diameter of less than 30 m will be considered as candidate asteroids, which in principle are unlike to represent a hazard. Accordingly, a Lambert arc in the Sun-centred two-body problem is utilised to estimate the asteroid capture windows and the first impulse used to manoeuvre the candidate asteroid from its initial orbit. Based on the initial guess from the first impulse, the transfer trajectory for the captured asteroid is propagated in the Sun-Earth circular restricted three-body problem. Then, two strategies to capture asteroids into bound orbits around the Earth after aerobraking will be considered. In the first case, the motion of the captured asteroid after aerobraking is modelled in the Earth-centred two-body problem and so a second impulse is required to raise the height of the perigee to avoid a second aerobraking pass. In the second case, the motion of the captured asteroid is still modelled in the Sun-Earth circular restricted three-body problem and the solar gravitational perturbation used to passively raise the height of the asteroid perigee, again avoiding subsequent aerobraking passes. The boundary of these two cases is the Earth's sphere of influence. Finally, the transfers are then optimised using a global optimisation algorithm and lists of candidate objects provided. We also note that while the strategies developed are applied to the capture of small near-Earth asteroids, they are also appropriate to the return of asteroid resources extracted in-situ and then transported via a carrier spacecraft.

2. Dynamical models

2.1 Circular restricted three-body problem

The Sun-Earth circular restricted three-body problem (CRTBP) provides a good approximation of the real Sun-Earth system [36] and is therefore introduced to describe the motion of a captured asteroid. In this model, it is assumed that the Sun and Earth move on a circular orbit around their common barycentre, shown in Fig. 1(a) and so the motion of the asteroid in the Sun-Earth rotating system is defined by [37]

$$\ddot{x} - 2\dot{y} = \frac{\partial \Omega}{\partial x}, \ddot{y} + 2\dot{x} = \frac{\partial \Omega}{\partial y}, \ddot{z} = \frac{\partial \Omega}{\partial z} \tag{1}$$

where

$$\Omega(x, y, z, \mu) = \frac{1}{2}[(x^2 + y^2) + \mu(1-\mu)] + \frac{1-\mu}{r_1} + \frac{\mu}{r_2}$$

and r_1 and r_2 are the distances of the candidate asteroid from the Sun and Earth respectively, scaled by the distance between the Earth and Sun (1 astronomical unit, AU). Moreover, $\mu = \mu_{Earth} / (\mu_{Sun} + \mu_{Earth})$ is the normalized mass parameter of the two primaries, assumed to be 3.036×10^{-6} for the Sun-Earth system [38]. For the circular restricted three-body problem, the Jacobi constant can be written as

$$C = 2\Omega(x, y, z, \mu) - (\dot{x}^2 + \dot{y}^2 + \dot{z}^2) \tag{2}$$

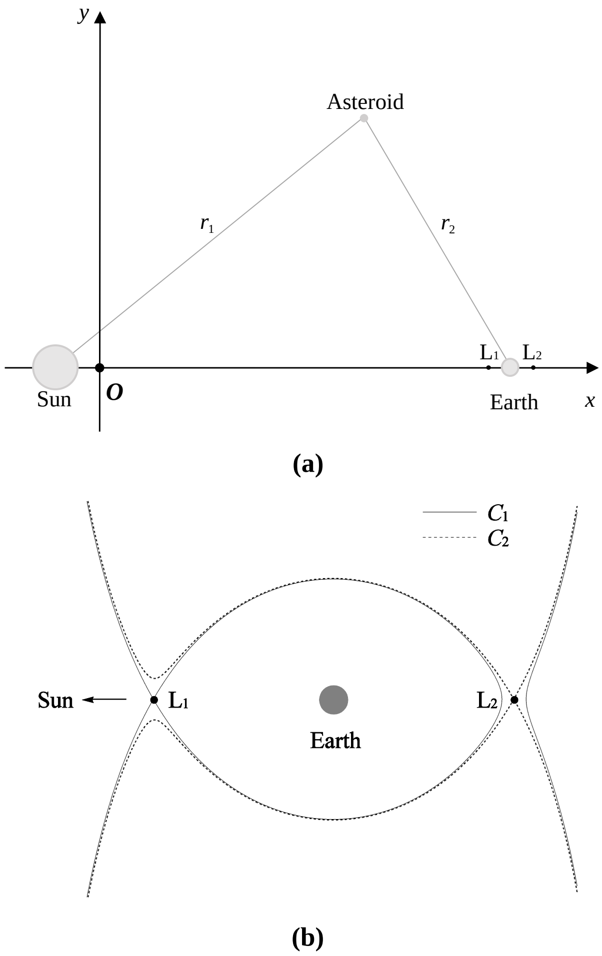

Fig. 1. (a) Geometry of the Sun-Earth circular restricted three-body problem; (b) x-y projection of the zero-velocity surface when $C = C_1$ and $C = C_2$.

There are then five libration points L_i, (i = 1-5) in the circular restricted three-body problem and the Jacobi constants at the libration points are denoted as C_i (i = 1-5). It should be noted that $C_1 > C_2 > C_3 > C_4 = C_5$. In the circular restricted three-body problem, the region of possible motion can be defined by the zero-velocity surface when $\dot{x}^2 + \dot{y}^2 + \dot{z}^2 = 0$. Figure 1(b) shows the *x-y* projection of the zero-velocity surface when $C = C_1$ and $C = C_2$. As shown in Fig. 1(b), for $C > C_1$, the region of possible motion is composed of three separate oval surfaces: two inner regions and one outer region. When $C = C_1$, the two inner oval regions merge at L_1 and then the inner and outer regions will merge when $C = C_2$. These conditions will be used later in Section 4 to determine the requirements for capture.

2.2 *Aerobraking model*

With a high relative velocity with respect to the Earth, a captured asteroid will pass through the Earth's atmosphere quickly and so would remain in the atmosphere for only a short duration. An approximate model can therefore be used where the aerobraking manoeuvre is modelled as a grazing hyperbolic fly-by. During the flyby, a first order approximation of the velocity change ($\Delta \boldsymbol{v}_a$) generated by the aerobraking manoeuvre can be written as [31]

$$\Delta \boldsymbol{v}_a = (1 - e^{B\rho\sqrt{2\pi r_p H_s (e+1)/e}})\boldsymbol{v}_{p-} \tag{3}$$

$$B = C_d \frac{A}{2M} \tag{4}$$

where $\boldsymbol{v}_{p-}$ is the relative velocity of the asteroid at perigee with respect to the Earth before aerobraking and C_d is the asteroid drag coefficient, assumed as a sphere as 0.47 [32]; A/M is the asteroid area-to-mass ratio; r_p is the perigee radius of the flyby orbit from the centre of the Earth and e is the eccentricity of the flyby orbit. In this model, it is assumed that the density of the atmosphere deceases exponentially from the Earth's surface and so can be written as

$$\rho = \rho_0 e^{-h/H_s} \tag{5}$$

where ρ_0 = 1.225 kg/m^3 is the density of the atmosphere at the surface and H_s = 7.249 km is the atmospheric scale height [39]. Assuming that the captured asteroid is a sphere with an average density ρ_a = 2600 kg/m^3[40], contour maps of the magnitude of the aerobraking manoeuvre imparted on the asteroid with respect to the asteroid's diameter D and the perigee height h above the Earth's surface are shown in Fig. 2.

Moreover, during the aerobraking manoeuvre, the energy loss due to the grazing pass through the upper atmosphere will be converted to the heat, and thus the aerobraking manoeuvre will lead to mass loss from the asteroid due to thermal ablation [41]. Therefore, it can be assumed that the mass loss of the asteroid should be a function of the change in the kinetic energy of the asteroid. Based on the approximate model for aerobraking in Eq. (3), the final mass m_+ of the candidate asteroid after aerobraking can be estimated as [32]

$$m_+ = m_- e^{\sigma(v_{p+}^2 - v_{p-}^2)/2} \tag{6}$$

where $\boldsymbol{v}_{p+} = \boldsymbol{v}_{p-} + \Delta\boldsymbol{v}_a$ is the relative velocity of the asteroid at perigee with respect to the Earth after aerobraking, m_- is the initial mass of the asteroid and σ is an ablation parameter, assumed to be 2.1×10^{-8} s^2/m^2 [32]. In fact, the ablation parameter σ is not a constant and can vary with the altitude of the aerobraking manoeuvre, the asteroid relative velocity and the size of the asteroid. Moreover, some large asteroids would suffer a lower level of ablation since the outer surface of the asteroid can act as an effective shield caused by a screening effect [42]. However, a constant value of the ablation parameter can provide an effective and conservative estimate of the asteroid's final mass [32]. Meanwhile, the mass loss ratio is defined by

$$f = \frac{m_- - m_+}{m_-} = 1 - e^{\sigma(v_{p+}^2 - v_{p-}^2)/2} \tag{7}$$

The ablation model will be used later in Section 3 for hazard analysis and Section 5 to optimise the capture strategy to maximise the final mass of the asteroid after the aerobraking manoeuvre.

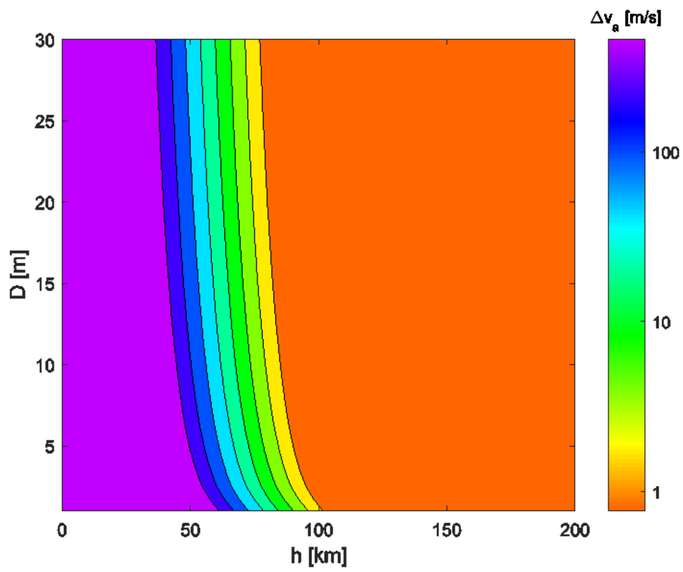

Fig. 2. Aerobraking manoeuvre Δv_a provided by the Earth's atmosphere as a function of height *h* and asteroid diameter *D*, when v_{p-} = 22 km/s.

Finally, using Eq. (3), the change in speed of the asteroid due to a grazing aerobraking manoeuvre can be determined. As shown in Fig. 2, we find that once the height *h* at perigee above the Earth's surface is larger than a critical value (approximately 100 km), the aerobraking manoeuvre can be neglected. Therefore, it is now assumed that the Earth's atmosphere cannot provide an aerobraking manoeuvre when $h > 100$ km. Accordingly, we now define $h_{threshold} = 100$ km as the height threshold for aerobraking above the Earth's surface.

3. Asteroid hazard analysis

When the candidate asteroid approaches the vicinity of the Earth, it poses a potential (if small) impact risk. Undoubtedly, the grazing atmospheric pass for aerobraking will increase the possibility of impact. Therefore, we should only consider those candidate asteroids which cannot in principle represent a threat. Since the Earth's atmosphere can disintegrate small bodies, and so acts as a shield, the candidate asteroids in this paper should be those asteroids which would also be disintegrated by the Earth's atmosphere. Most asteroids with diameter of less than 50 m are thought to break up in the atmosphere and cannot reach the surface [43, 44]. Besides, Vasile and Colombo [45] regarded 40 m as the critical threshold above which the Earth's atmosphere will no longer disintegrate an asteroid. Moreover, other authors have noted that the atmosphere can protect against the asteroids with diameter less than 30 m [46, 47]. Therefore, to reduce the threat of impact with the Earth, we only consider small asteroids with $D < 30$ m as candidates for aerobraking in this paper, although clearly detailed risk assessment is required. In addition, if a mission to capture an asteroid with a diameter of 30 m fails and the asteroid's height at perigee with respect to the Earth is small enough to pose a threat of impact, the final mass of the asteroid after atmosphere entry and ablation can be estimated from Eq. (6). Figure 3 shows the mass loss ratio of a 30-m asteroid after aerobraking with a range of incident velocities relative to the Earth and a number of (low) perigee heights h with respect to the Earth's surface. As shown in Fig. 3, the aerobraking manoeuvre at low perigee heights (especially $h < 40$ km) can lead to significant mass loss, thereby potentially mitigating further risks of impact of the asteroid. However, the use of the analysis of Section 2.2 is clearly only approximate and we note that complete ablation in the atmosphere may still lead to surface damage due to shock wave propagation [48].

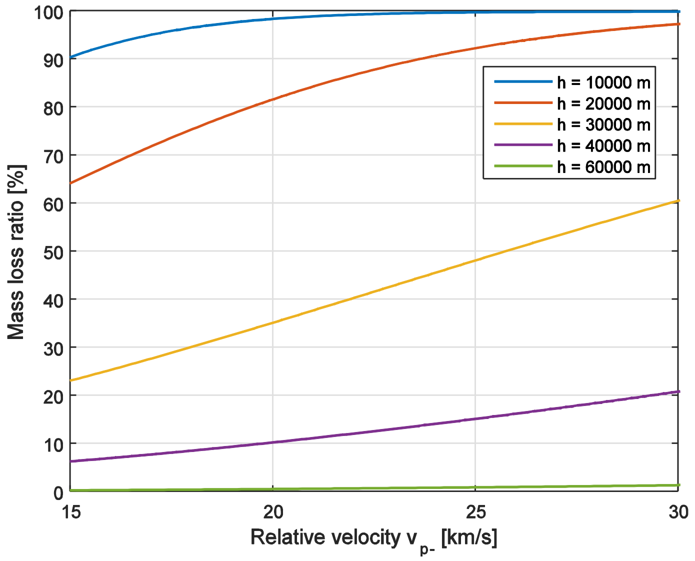

Fig. 3 Mass loss ratio of a 30-m asteroid after aerobraking with incident velocity with respect to the Earth

Furthermore, the natural average impact interval for asteroids can be estimated by an empirical scaling law [49]

$$T_{impact}[\mathrm{y}] = 3.71 \times 10^{-2} D[\mathrm{m}]^{2.377} \tag{8}$$

where the time interval is measured in years and the asteroid diameter is provided in meters. Figure 4 shows the corresponding natural average impact interval of asteroids with respect to the asteroid's diameter. As shown in the Fig.4, the average impact interval for a 30-m asteroid is approximately 1 century. Therefore, the risk of capturing a similar body will add to the natural background risk, although again the risk is in principle small. It can also be considered that dis-assembling an asteroid prior to encounter, with a number of smaller fragments aerobraking individually, can reduce risks further. Finally, if it is assumed that the asteroid is a homogeneous spherical object with density ρ_a then the diameter of the asteroid can be estimated as

$$D[\mathrm{m}] = 1329\mathrm{km} \times 10^{-H/5} p_v^{-1/2} \tag{9}$$

where H is the absolute magnitude of the asteroid and p_v is its albedo. Here we assume that the asteroids have a typical albedo of p_v = 0.154 [40]. Considering D < 30 m, the candidate asteroids should therefore be those with an absolute magnitude H > 25.26.

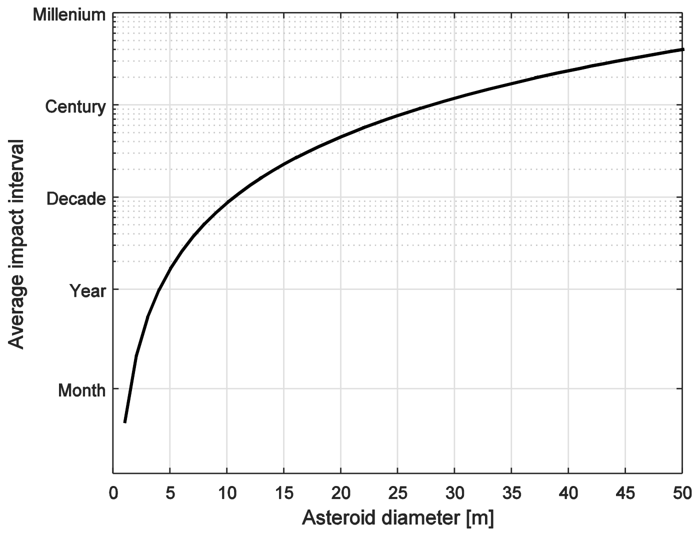

Fig. 4. Estimated average natural impact interval of asteroids versus asteroid diameter

4. Asteroid capture around the Earth using aerobraking

The strategy for capturing an asteroid into a bound orbit around the Earth using an aerobraking manoeuvre is illustrated in Figure 5. With an initial manoeuvre $\Delta \boldsymbol{v}_1 = \Delta v_1 \left[\sin\theta_1 \cos\theta_2, \sin\theta_1 \sin\theta_2, \cos\theta_1\right]^T$ with $\theta_1 \in [0,\pi]$ and $\theta_2 \in [0,2\pi]$, referring to a local spherical reference frame along the asteroid's orbit where the *x* axis is along the asteroid's velocity vector, the *y* axis is perpendicular to the *x*-axis and in the plane of the asteroid orbit and the *z* axis is normal to the plane of the asteroid orbit, the candidate asteroid leaves from its initial orbit and its motion can then be described by the Sun-Earth circular restricted three-body problem, as detailed in Section 2.1. Subsequently, the candidate asteroid performs an aerobraking manoeuvre and is thus captured into a bound orbit about the Earth.

The Jacobi constant of the captured asteroid after aerobraking is denoted as C_+ . According to the capture condition [50], the candidate asteroid is assumed to be ballistically captured to Earth orbit if

$$H_2 < 0 \tag{10}$$

where H_2 is the two-body Kepler energy of the asteroid after aerobraking and can be written as

$$H_2 = \frac{1}{2} {v_{p+}}^2 - \frac{\mu_{Earth}}{r_p} \tag{11}$$

More specifically, the candidate asteroid is considered to be captured temporarily around the Earth if $v_{p+} < \sqrt{2\mu_{Earth} / r_p}$ and $C_+ < C_1$. Similarly, the asteroid can be captured permanently in the Earth's Hill region if $v_{p+} < \sqrt{2\mu_{Earth} / r_p}$ and $C_+ > C_1$ [16]. For the temporary capture case, the captured asteroid may orbit the Earth for a long duration before it escapes from the vicinity of the Earth. Therefore, this capture strategy can still be practical. Thus, the asteroid capture strategy presented in this paper contains both temporary capture and permanent capture. That is, once $v_{p+} < \sqrt{2\mu_{Earth} / r_p}$, the candidate asteroid is considered to be captured to Earth orbit.

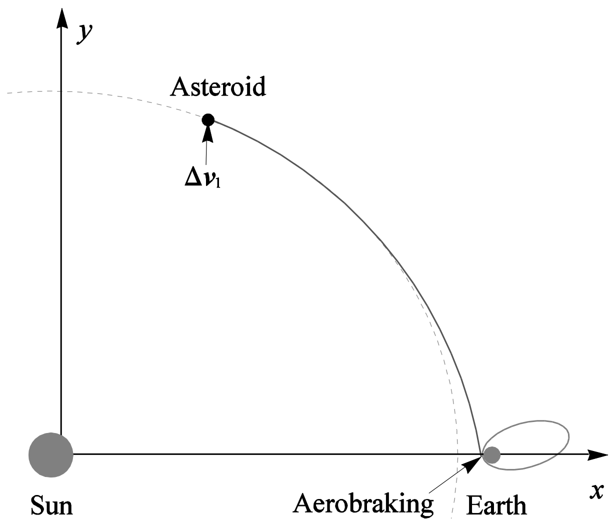

Fig. 5. Overview of capturing near-Earth asteroids to Earth orbit using aerobraking

4.1 *Asteroid capture opportunities and initial guess*

For each candidate asteroid, feasible capture dates (T_0) are assumed to be in the interval 2019–2050 (or 58484 MJD - 70171 MJD). It is also assumed that the asteroid orbital elements remain unchanged within its current synodic period with respect to the Earth. We define this time period (in the interval 2019–2050) during which the asteroid orbital elements are valid as the asteroid capture window.

The Lambert arc between the candidate asteroid's initial orbit and the Earth in the Sun-centred two-body problem can be used as an initial guess of the capture date T_0 and the first impulse $\Delta \boldsymbol{v}_1$. In addition, the first manoeuvre of this Lambert arc in the Sun-centred two-body problem is denoted as $\delta \boldsymbol{v}_1$. Here a flight time T_{fly} < 2000 days is considered and then the first impulse $\delta \boldsymbol{v}_1$ on the Lambert arc is utilised to guess the first impulse $\Delta \boldsymbol{v}_1$ in the Sun-Earth CRTBP. Since we expect to find the candidate asteroids which can be captured with low cost, here we set 50 m/s as a threshold for δv_1. Moreover, we only consider those asteroids with a diameter D less than 30 m, as noted in Section 3. Therefore, those asteroids with $\delta v_1 \leq 50\,\text{m/s}$ and $D < 30$ m ($H > 25.26$) are then considered to be candidate asteroids, as shown in Fig. 6, where the JPL Small-Body Database has been used[1]. For a suitable candidate asteroid, the departure date on the Lambert arc with $\delta v_1 \leq 50\,\text{m/s}$ can then be used as an approximation of the capture date T_0 when the first impulse $\Delta \boldsymbol{v}_1$ is applied to the candidate asteroid, as shown for 2005 VL1 for illustration in Fig. 7.

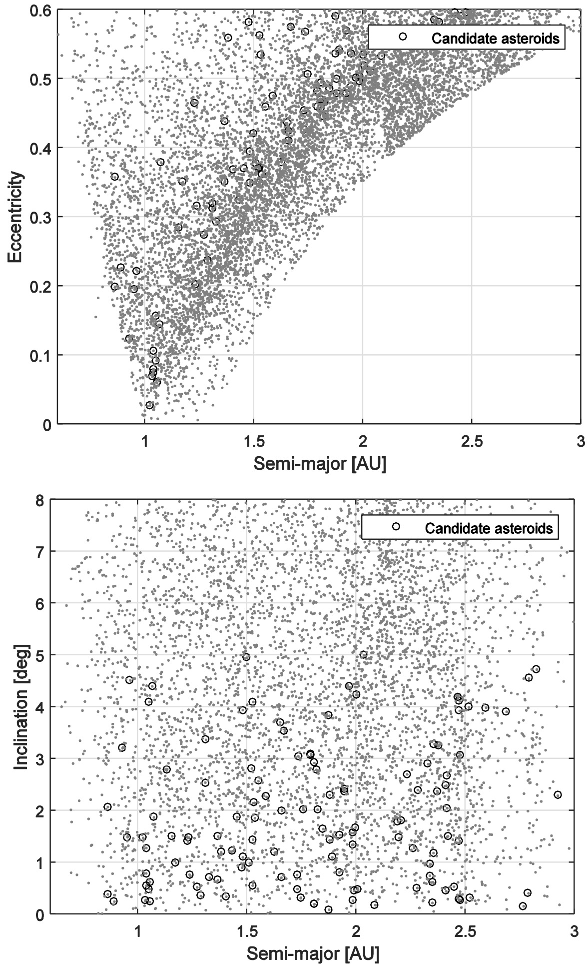

Fig. 6. Distribution of candidate asteroids (circled) in the family of near Earth asteroids.

[1] https://ssd.jpl.nasa.gov/?sb_elem

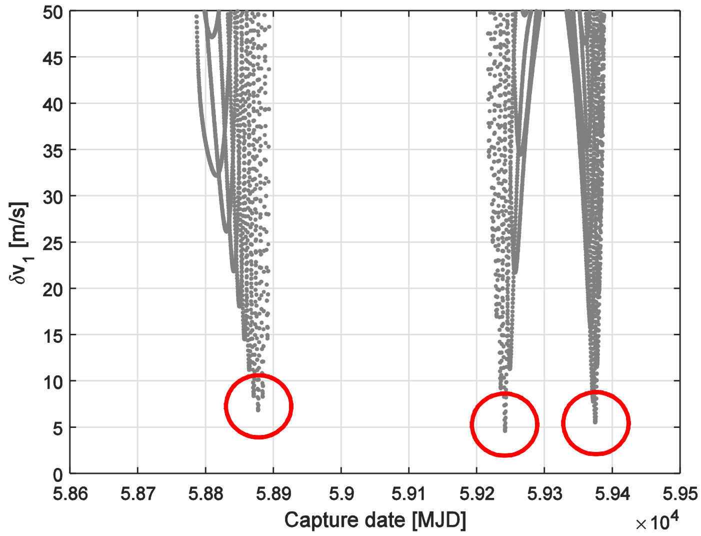

Fig. 7. Optimal capture date T_0 guess for capturing 2005 VL1 with potential capture dates highlighted.

4.2 Two approaches to raise the perigee height after aerobraking

In order to simplify the capture strategy, only a single aerobraking manoeuvre is utilised to capture asteroids to Earth orbit in this paper. Therefore, strategies to raise the perigee height of the asteroid orbit soon after aerobraking are required, with the new perigee height (h) above the Earth's surface being more than 100 km. Here, two methods of raising the perigee height after aerobraking are proposed, corresponding to the two different dynamical models after the aerobraking manoeuvre.

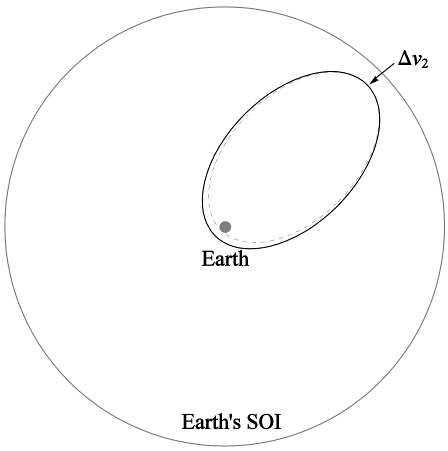

(a)

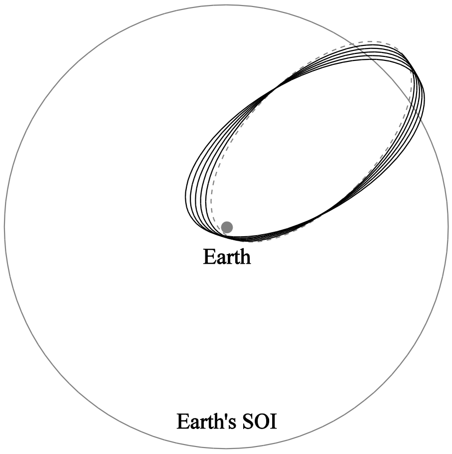

(b)

Fig. 8. Strategies to raise the perigee height after aerobraking: (a) additional manoeuvre at apogee; (b) three-body interaction.

After aerobraking, if the captured asteroid moves around the Earth inside the Earth's sphere of influence, it is assumed that the candidate asteroid is captured in a bound orbit around the Earth, and so an Earth-centred two-body analysis can be used. Hence, the state of the captured asteroid after aerobraking $\boldsymbol{v}_{p+}$ should be propagated forward in the Earth-centred two-body problem until it reaches the apogee. At apogee, a second impulse $\Delta\boldsymbol{v}_2$ is applied to the asteroid in order to raise the next perigee (h > 100 km), as shown in Fig. 8(a). In this strategy, two manoeuvres are therefore required to capture the candidate asteroid into a suitable bound orbit around the Earth.

Instead, for orbits with a large post-aerobraking apogee the state of the captured asteroid after aerobraking should be propagated forward in the Sun-Earth CRTBP model and an alternative strategy can be devised. With the gravitational perturbation due to the Sun, the orbit of the captured asteroid will deviate from a Keplerian ellipse. In general, the Sun's perturbation will modify the orbital elements of a body around the Earth, including the semi-major, eccentricity and inclination, etc. [51]. Accordingly, the perigee height above the Earth's surface will change. This provides opportunities to raise the perigee height of a captured asteroid orbit after aerobraking. Hence the gravitational perturbation of the Sun can in principle be utilised to passively raise the asteroid perigee height after aerobraking. Therefore, only one manoeuvre is in principle required to capture the candidate asteroid to Earth orbit, as shown in Fig. 8(b). In this strategy to raise the perigee height of the asteroid orbit, the Sun's gravity can be regarded as a disturbing perturbation to an Earth-centred two-body orbit and thus the short-term change of the perigee height of the asteroid orbit can be estimated by investigating the change in the asteroid's Earth-centred orbital elements using the Lagrange planetary equations [51]. Here we denote the eccentricity, inclination, right ascension of the ascending node, argument of perigee and true anomaly of the asteroid after aerobraking as e_+, i, Ω, ω and θ respectively, shown in Fig. 9. When the asteroid is at the perigee of its orbit around the Earth, $\theta = 0$, the change in the height of next perigee (after 1 revolution) can be estimated using [51]:

$$\delta h = \frac{5\pi e_+}{n^2}\sqrt{\frac{1+e_+}{1-e_+}}K_p \tag{12}$$

$$K_p = \frac{3\mu_{Sun}}{r_{sp}^{\ 3}} r_p (AB\cos(2\omega) - 0.5(A^2 - B^2)\sin(2\omega)) \tag{13}$$

where $A = \cos(\Omega - \theta_{SE})$, $B = -\cos i \sin(\Omega - \theta_{SE})$ and r_{sa} is the distance between the candidate asteroid at perigee when aerobraking and the Sun; n is the mean angular motion of the captured asteroid around the Earth; θ_{SE} is the angle of the Sun with respect to the Earth, measured from the positive x axis in an Earth-centred inertial frame XYZ, shown in Fig. 9.

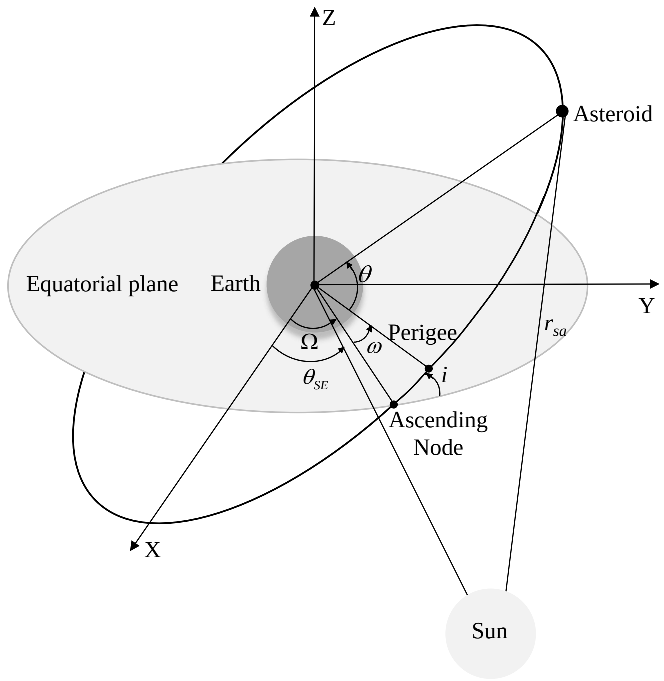

Fig. 9. Geometry of the captured asteroid and the Sun in the Earth-centred inertial frame XYZ.

It should be noted that Eq. (12) provides an approximation to the change in the height of the next perigee after aerobraking and thus it will be different from the true change of the next perigee height in the Sun-Earth CRTBP model. However, we can still use the sign of the term K_p in Eq. (12) as a fundamental filter for the solution space in the following optimisations. That is, results with $K_p < 0$ will be discarded from the solution space before checking whether the height of new perigee above the Earth's surface is larger than 100 km or not in the following optimisation. This filter will discard capture orbits where the solar gravitational perturbation lowers the perigee further, rather than passively raises the perigee above 100 km.

4.3 Bi-impulse capture of asteroids to Earth orbit

As shown in Fig. 8(a), for the bi-impulse capture strategy, it is assumed that the captured asteroid moves in a bound orbit around the Earth inside the Earth's sphere of influence and so the state of the captured asteroid after aerobraking can be propagated forward in the Earth-centred two-body problem. Hence, capture of the asteroid to Earth orbit is defined here by

$$\begin{cases} v_{p+} < \sqrt{2\mu_{Earth} / r_p} \\ r_a < r_{SOI} \end{cases} \tag{14}$$

where r_a is the distance from the centre of the Earth to the apogee of the captured asteroid's orbit after aerobraking and r_{SOI} = 925000 km is the radius of the Earth's sphere of influence. Then, a second impulse is required to raise the subsequent perigee of the trajectory after aerobraking out of the Earth's atmosphere so that the distance from the centre of the Earth to the new perigee of the asteroid's orbit should be

$$r_{np} \geq 6378 + 100 = 6478 \text{ km} \tag{15}$$

Therefore, the second impulse which is required to raise the orbit perigee can be written as

$$\Delta v_2 = \frac{h_a}{r_a} - \frac{\sqrt{r_a \mu_{Earth}(1-e_n)}}{r_a} \tag{16}$$

where h_a is the magnitude of asteroid's angular momentum before aerobraking; e_+ is the eccentricity of post-aerobraking orbit; e_n is the eccentricity of the orbit with the raised perigee and

$$h_a = r_p \left|\boldsymbol{v}_{p+}\right|, \ e_+ = \frac{h_a^{\ 2}}{r_p \mu_{Earth}} - 1, \ r_a = \frac{h_a^{\ 2}}{\mu_{Earth}(1-e_+)}, \ e_n = \frac{r_a - r_{np}}{r_a + r_{np}}$$

The minimum value of Δv_2 can be obtained when $r_{np} = 6478km$. Therefore, the total cost of capturing an asteroid around the Earth using this capture strategy is given simply by

$$\Delta v = \Delta v_1 + \Delta v_2 \tag{17}$$

In this capture strategy, for one candidate asteroid, as shown in Fig. 6, there are 4 parameters: (T_0, Δv_1, θ_1, θ_2). However, a uniform random sampling of θ_1 and θ_2 cannot result in a uniform distribution of points in the solution space [52]. Therefore, a transformation of θ_1 and θ_2 is required such that [53]

$$\begin{cases} \theta_1 = 2\pi\alpha, & \alpha \in [0,1] \\ \theta_2 = \cos^{-1}(2\beta - 1), & \beta \in [0,1] \end{cases} \tag{18}$$

Therefore, this problem can be transformed to a problem with 4 parameters: (T_0, Δv_1, α, β). These transfer trajectories can be searched using a global optimisation method NSGA-II [54], using the total Δv cost as the objective function and Eq. (14) as the constraints. Then transfers obtained with NSGA-II can be locally optimised with sequential quadratic programming (SQP), implemented in the function *fmincon* in MATLAB. Therefore, a list of asteroids which can be captured with a total Δv cost of less than 50 m/s is shown in Table 1. An example of a transfer trajectory to capture 2005 VL1 is shown in Fig. 10.

As shown in Table 1, the asteroid capture strategy using aerobraking can achieve low-energy capture of asteroids, especially for 2005 VL1, 2008 EK68, 2009 WD54 and 2012 BV1. Amongst them, the lowest cost transfer is below 10 m/s, corresponding to the capture of 2005 VL1 into a bound orbit around the Earth. Comparing the results of the two manoeuvres in Table 1, we find that most of the second (perigee raising) manoeuvres are much smaller than the first manoeuvre. That is, for asteroid capture missions using aerobraking, most propellant will be consumed to manoeuvre the candidate asteroid from its initial orbit. Although aerobraking can enable low-energy capture of small asteroids, the accompanying mass loss of the captured asteroid due to atmospheric ablation may be high, as determined from Eq. (7). For example, over half of 2008 EK68's mass would be lost during the aerobraking when the total Δv cost alone is used as the objective function for the optimisation problem. Therefore, an asteroid capture mission with minimum total Δv cost may not be economically optimal, as will be discussed later in Section 5.

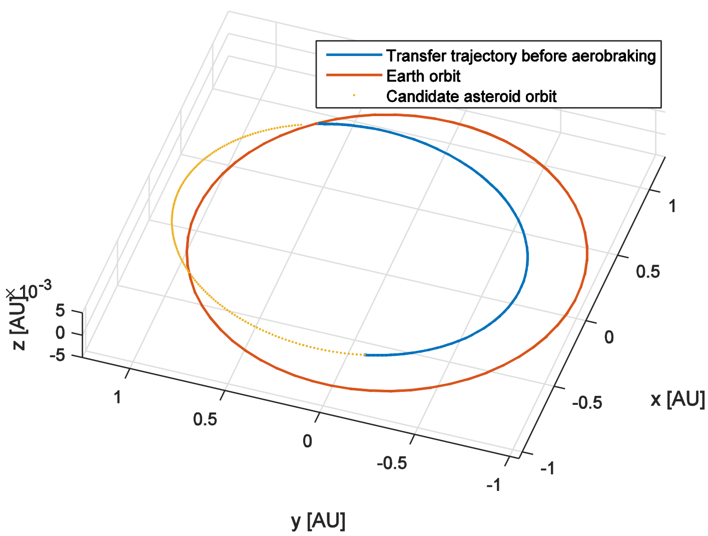

(a)

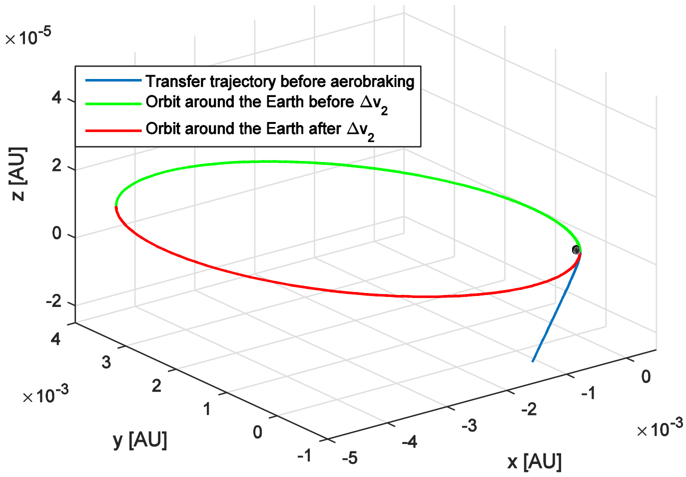

(b)

Fig. 10. Transfer trajectory capturing 2005VL1 including: a) transfer trajectory before aerobraking in the Sun-centred inertial frame; b) orbit around the Earth after aerobraking in the Earth-centred inertial frame.

Table 1 Optimal results of capturing asteroids around the Earth in the Earth two-body problem

Asteroid	Diameter, D	Capture date T_0, MJD	Flight time, day	Total cost, m/s	First impulse Δv_1, m/s	Second impulse Δv_2, m/s	Mass loss f, %
1998 KY26	26.9	60365.8	109	37.5	37	0.5	14.6
2003 YS70	5.1	59779.6	146.1	20.5	20.1	0.4	16.7
2005 TH50	8.5	60578	1467.7	48.4	47.4	1.1	20.7
2005 VL1	13.5	59372.6	143.2	5.4	4.8	0.6	31.2
2007 UD6	7.4	63224.7	659.2	16.4	15.8	0.6	29.3
2008 EK68	4.1	60608.8	496.9	6.3	5.4	0.9	59.3
2008 UA202	4.5	60862.7	1561.2	42.6	41.2	1.5	7.7
2008 WM61	15.5	59891.9	1472.9	31.6	31	0.7	27.6
2009 WD54	6.8	61065.9	1393.2	8.5	8	0.6	39
2010 TW54	10.2	60067.8	1248.9	34.9	32.9	2.1	45.4
2010 UY7	6.8	60111.1	1591.9	33.2	32.8	0.4	11.8
2010 VO21	6.2	63807.1	1189.6	30.2	29.4	0.7	21
2010 XT10	17	61917.9	190.4	49.5	49.1	0.4	24.8
2012 BV1	2.1	59596.5	362.6	8.5	8	0.5	53.8

2012 EP10	5.1	60810	292.7	18.6	18	0.6	12.3
2012 HG2	13.5	59673.1	1035	33.3	32.9	0.4	12.9
2012 VC26	6.2	59518.6	1467.8	45	40.8	4.2	35.5
2013 GM3	18.6	59695.8	1447.9	38.5	37.2	1.4	39.6
2014 GQ17	12.9	62034	195.4	45.6	45.1	0.5	30.4
2014 JR24	4.7	59115.7	1692.4	17.8	17.4	0.4	11.5
2014 QN266	18.6	59752.6	1723.8	31.3	30.8	0.5	7
2014 WE6	2.8	63515.7	1130.2	24.2	23.2	1	17.2
2015 PS228	5.5	62171.8	1617.4	49.6	49	0.6	7

4.4 Single impulsive capture of asteroids around the Earth

As shown in Fig. 8(b), in this capture strategy, the state of the captured asteroid after aerobraking should be propagated forward in the Sun-Earth circular restricted three-body problem. Here we assume that the captured asteroid moves away from the vicinity of the Earth such that the perigee of the captured asteroid is outside the Earth's sphere of influence. Therefore, capture of the asteroid can be defined here by

$$\begin{cases} v_{p+} \le \sqrt{2\mu_{Earth} / r_p} \\ \min(r_{p+}) > 6478\,\text{km} \\ \max(r_{p+}) < r_{SOI} \end{cases} \tag{19}$$

where $\min(r_{p+})$ is the minimum perigee distance to the centre of the Earth after aerobraking and $\max(r_{p+})$ is the maximum perigee distance after aerobraking within a given post-aerobraking duration (1000 days). It should be noted that even though the new perigee height above the Earth's surface can be raised to be more than 100 km, the Earth's atmosphere can still provide a small drag force at subsequent perigee passages and thus would act as a perturbation to the asteroid orbit. Considering the sensitivity of orbit in the Sun-Earth circular restricted three-body problem, we should take this perturbation into account within a given post-aerobraking duration (1000 days) which can be estimated using Eq. (3). Here, the total cost of capturing the asteroid about the Earth is given simply

$$\Delta v = \Delta v_1 \tag{20}$$

In this capture strategy, for one candidate asteroid in Fig. 6, there are also 4 parameters: (T_0, Δv_1, α, β). These transfer trajectories can again be searched using NSGA-II, using the total Δv cost as the objective function and Eq. (19) as the constraints. Then transfers obtained with NSGA-II can be locally optimised with the function *fmincon* in MATLAB Therefore, the list of asteroids that can be captured with a total Δv cost below 50 m/s is shown in Table 2. An example of a transfer trajectory is shown in Fig. 11-12. As shown in Fig. 12, it can be seen that the perigee height (red points) of the captured asteroid orbit after aerobraking can be passively raised using the gravitational perturbation of the Sun, in this case for 1000 days. This demonstrates that that a second aerobraking pass cannot occur within 1000 days after the initial aerobraking for asteroid capture. To investigate the long-term dynamical behaviour of the capture orbit after aerobraking, and to determine when a second aerobraking pass will occur, we propagate the capture orbit of 2005VL1 at the Earth for 6000 days after aerobraking. The time history of the perigee height of the captured asteroid's orbit above the Earth's surface with respect to flight time is shown in Fig. 13. It can be seen the perigee of the captured asteroid orbit remains inside the Earth's sphere of influence for 6000 days. Moreover, the perigee height of the captured asteroid orbit at the Earth increases continuously within approximately 3000 days after the aerobraking manoeuvre. Then, due to the long-term influence of the Sun's gravitational perturbation, the perigee height of the captured asteroid orbit is lowered gradually after a significant further duration (about 3000 days). Consequently, a second aerobraking phase may occur 6000 days after the initial aerobraking for asteroid capture. Nevertheless, before the second aerobraking phase, there is in principle sufficient time to explore and exploit the captured asteroid and its resources.

Similar to the bi-impulse capture strategy, aerobraking can again save significant energy and thus can enable the low-cost capture of a number of asteroids in the Sun-Earth circular restricted three-body problem. Since no further manoeuvre is required to raise the perigee height after aerobraking, the total cost of this capture strategy is slightly smaller than the bi-impulse capture strategy in the Earth-centred two-body problem. For example, the cheapest transfer in this capture strategy also corresponds to a capture of 2005 VL1, and its total cost is only 0.5 m/s smaller than that of the bi-impulse capture strategy. To further illustrate this dynamical behaviour shown in Fig. 13, we define the change in the height between one perigee and the previous perigee along the asteroid orbit around the Earth as the following:

$$\Delta h_j = h_j - h_{j-1}\,,\ \ j = 1,2,3... \tag{21}$$

where h_j is the height of j^{th} perigee with respect to the centre of the Earth after aerobraking and h_0 is the perigee height when aerobraking. Moreover, using the approximation in Eq. (12), the estimated change in the height between one perigee and the previous perigee can be written as

$$\delta h_j = (h_{j-1} + \delta h) - h_{j-1}, \;\; j = 1, 2, 3... \tag{22}$$

where δh_j is estimated change in height between the j^{th} perigee and the $(j-1)^{th}$ perigee using Eq. (12), based on the true orbital elements at the $(j-1)^{th}$ perigee. The comparison of the true change and estimated change in the perigee height is shown in Fig. 14. The slight differences between the true change and estimated change demonstrates the validity of the approximation in Eq. (12). Furthermore, the change in the perigee height has clear periodicity and it exhibits a long-period variation, as discussed earlier.

One of the main challenges of the two capture strategies is the sensitivity of the transfer trajectory of the candidate asteroid, since small perturbations or impulse manoeuvre errors would result in the failure of the aerobraking manoeuvre. Therefore, an accurate and robust navigation and control strategy would be required to guarantee that the candidate asteroid encounters the Earth with the correct perigee height to achieve the required aerobraking manoeuvre for capture. It is envisaged that the transfer vehicle used to provide the initial manoeuvre of the asteroid would remain attached to it, thereby allowing mid-course corrections. In principle, depending on the size of the asteroid and transfer vehicle, the vehicle could remain attached during aerobraking, with the asteroid body protecting the vehicle. This would also allow the perigee raising manoeuvre to be performed on the first orbit after aerobraking.

Another challenge is the uncertainty of the properties of the candidate asteroid. Aerobraking can cause mass loss of the asteroid due to ablation which depends on the asteroid’s geometry, material properties and composition. A suitable heat shield, potentially an inflatable structure, or manufactured from the asteroid material itself, could provide protection of the candidate asteroid and thereby reduce ablative mass loss during aerobraking, while improving the predictability of the aerobraking manoeuvre.

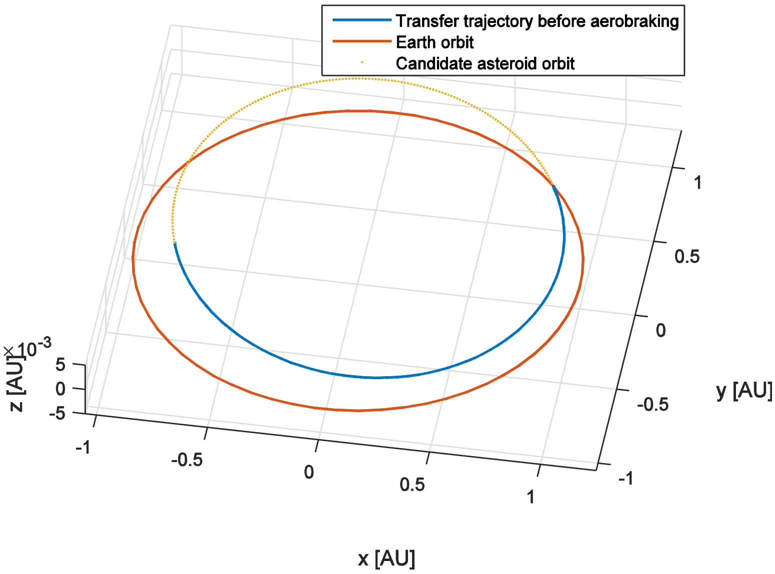

Fig. 11. Transfer trajectory of capturing 2005VL1 before aerobraking in the Sun-centred inertial frame.

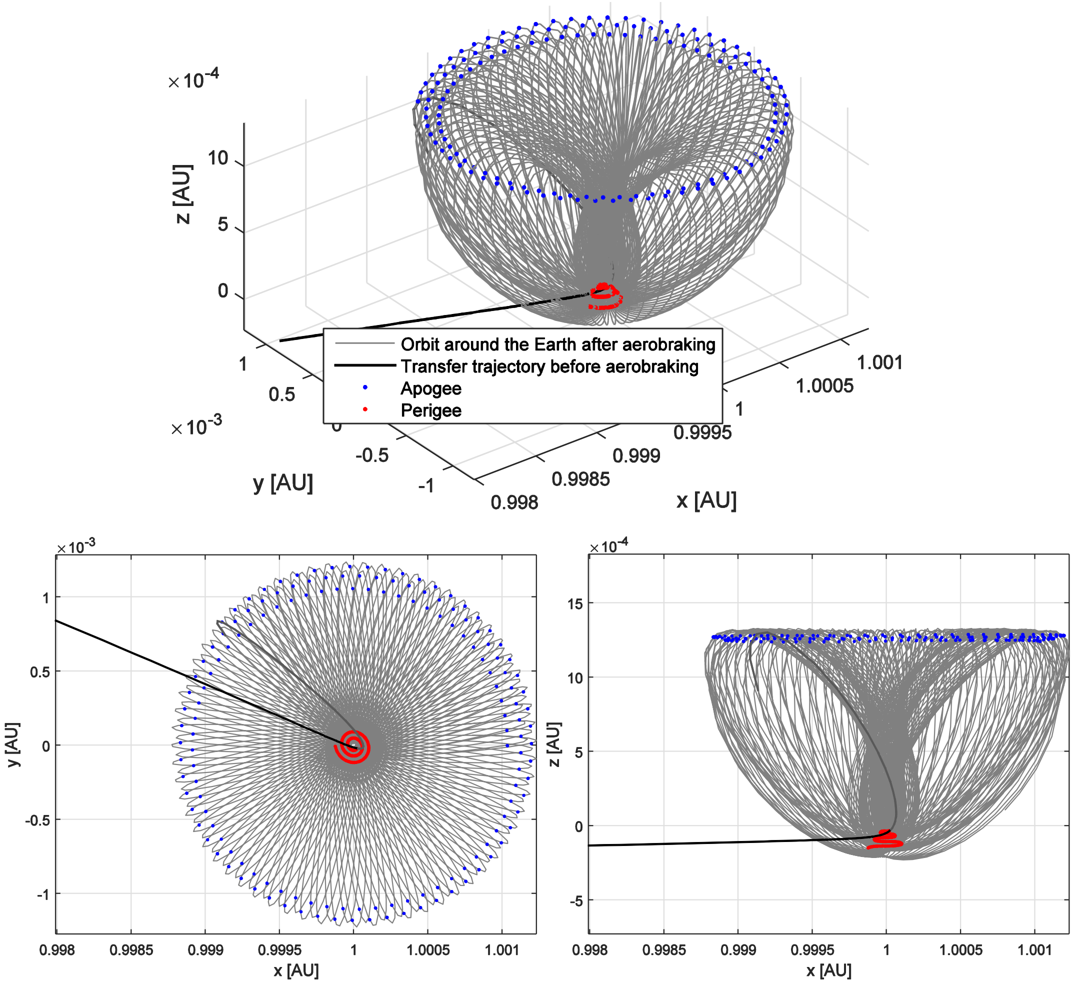

Fig. 12. Capture orbit of 2005VL1 around the Earth after aerobraking for 1000 days in the Sun-Earth rotating frame.

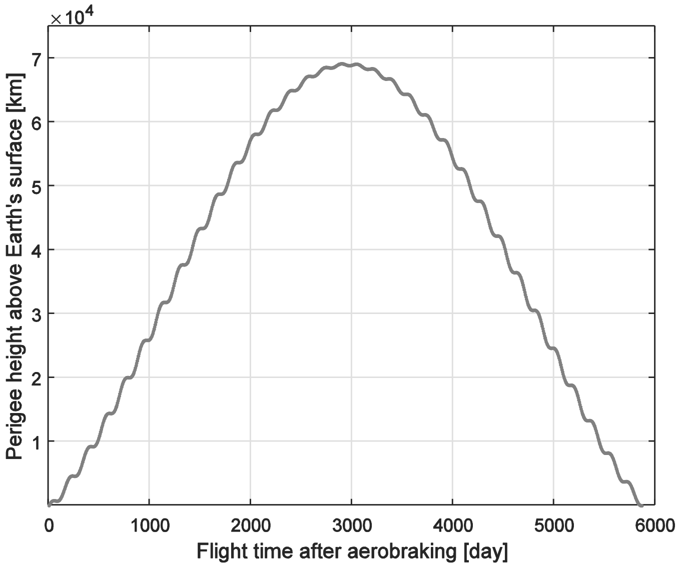

Fig. 13. Perigee height of the captured asteroid's orbit around the Earth after aerobraking

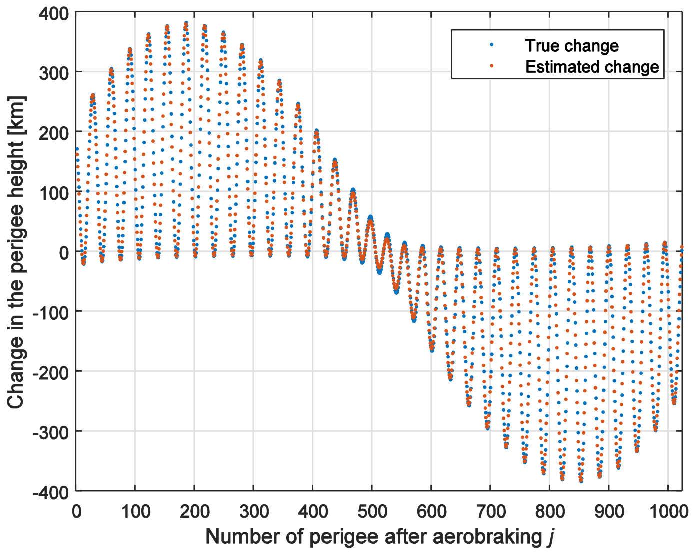

Fig. 14. Comparison of the true change and estimated change in the perigee height.

Table 2 Results of capturing asteroids around the Earth in the Sun-Earth CRTBP

Asteroid	Diameter, D	Capture date T_0, MJD	Flight time, day	Total cost, m/s	Mass loss *f*, %
1998 KY26	26.9	60368.4	107.3	40.4	16.2
2003 YS70	5.1	59779.3	146.5	19.3	19.7
2005 TH50	8.5	60582	1463.7	47.6	19.7
2005 VL1	13.5	59372.5	143.3	4.9	30.5

2007 UD6	7.4	63218.2	665.7	15.5	29.3
2008 EK68	4.1	60608.2	497.5	5	59.1
2008 UA202	4.5	60874.3	1549.6	40.7	4.7
2008 WM61	15.5	59888.8	1476.3	34.2	26.9
2009 WD54	6.8	61056.8	1402.7	7.8	39
2010 TW54	10.2	60075	1241.9	31.8	44.2
2010 UY7	6.8	60108.6	1594.3	31.1	12.6
2010 VO21	6.2	63809.6	1187.3	29.3	21.4
2010 XT10	17	61905.3	203.7	39.8	28.1
2012 BV1	2.1	59595.3	364.2	7.8	54.5
2012 EP10	5.1	60808.5	294.1	18.1	14.3
2012 HG2	13.5	59668.1	1040.1	33.1	17.1
2012 VC26	6.2	59527.5	1458.8	41.4	29.8
2013 GM3	18.6	59692.9	1450.9	38.6	40.1
2014 GQ17	12.9	62043.7	185.5	44.7	32.4
2014 JR24	4.7	59106.5	1702	17.2	12.8
2014 QN266	18.6	59752.6	1723.8	31.3	7
2014 WE6	2.8	63515.7	1130.2	24.2	17.2
2015 PS228	5.5	62171.8	1617.4	49.6	7

5. Maximum mass ratio of the captured asteroid and spacecraft

From an economic point of view, we should take the mass of the spacecraft required to capture the candidate asteroid into account. Moreover, to measure the yield of the asteroid capture mission, the ratio of the mass of the captured asteroid (after aerobraking to the mass of the transfer vehicle is defined as

$$f_m = \frac{m_+}{m_0} \tag{23}$$

where m_0 is the (wet) mass of the transfer vehicle at rendezvous with the candidate asteroid, and again m_+ is the final mass of the asteroid after aerobraking. It is assumed that a minimum of 20% of the mass of the transfer vehicle is allocated to structure and subsystems and that its specific impulse is I_{sp}= 300 s (bi-propellant engine).

For the bi-impulse capture strategy, after the first impulse Δv_1, the spacecraft's mass is then

$$m_1 = (m_- + m_0)e^{-\Delta v_1/(gI_{sp})} - m_- \tag{24}$$

and then after second impulse Δv_2 ,the spacecraft's mass becomes

$$m_2 = ((m_- + m_0)e^{-\Delta v_1/(gI_{sp})} - m_- + m_+)e^{-\Delta v_2/(gI_{sp})} - m_+ \tag{25}$$

again where m_- is the initial mass of the asteroid prior to aerocapture. Thus, we have

$$((m_- + m_0)e^{-\frac{\Delta v_1}{gI_{sp}}} - m_- + m_+)e^{-\frac{\Delta v_2}{gI_{sp}}} - m_+ \geq 0.2m_0 \tag{26}$$

Hence, the minimum (wet) mass of the spacecraft required to capture the target asteroid can be written as

$$m_0 = \frac{(m_- - m_+)e^{-\Delta v_2/(gI_{sp})} + m_+ - m_- e^{-\Delta v/(gI_{sp})}}{e^{-\Delta v/(gI_{sp})} - 0.2} \tag{27}$$

Therefore, after substituting Eq. (6) into Eq. (25), the mass ratio of the captured asteroid after aerobraking and the required spacecraft mass can be written as

$$f_m = \frac{e^{-\Delta v/(gI_{sp})} - 0.2}{(e^{-\sigma(v_{p+}^2 - v_{p-}^2)/2} - 1)e^{-\Delta v_2/(gI_{sp})} + 1 - e^{-\Delta v/(gI_{sp}) -- \sigma(v_{p+}^2 - v_{p-}^2)/2}} \tag{28}$$

where the ablative mass loss of the asteroid has been accounted for. On the other hand, for the single impulsive asteroid capture strategy, the mass ratio of the captured asteroid after aerobraking and the required spacecraft mass is given by

$$f_m = \frac{e^{-\Delta v/(gI_{sp})} - 0.2}{1 - e^{-\Delta v/(gI_{sp}) -- \sigma(v_{p+}^2 - v_{p-}^2)/2}} \tag{29}$$

In these two capture strategies, for each candidate asteroid, there are again 4 variables: (T_0, Δv_1, α, β). The same list of asteroids in Table 1 and Table 2 is investigated and the optimal transfers for capturing those asteroids around the Earth using aerobraking can again be obtained with NSGA-II using Eq. (28) or Eq. (29) as the objective function. Therefore, the new optimal results are shown in Table 3 and Table 4.

From Table 3 and Table 4, we note that the retrieved masses of the captured asteroids using aerobraking are over tens of times more than that of the spacecraft that is required to execute the mission, particularly for 2005 VL1, 2008 EK68, 2009 WD54 and 2012 BV1. Comparing the results of Table 1-4, the asteroids with smaller total Δv cost in Table 1 and Tables 2 can be potentially captured with a larger ratio of the retrieved mass to the required spacecraft mass. However, minimum total Δv cost does not always imply the maximum yield of a retrieval mission. For example, the mass ratio f_m for capturing 2009 WD54 is larger than that of capturing 2008 EK68, while the total Δv cost of capturing 2008 EK68 is smaller than that of capturing 2009 WD54. Furthermore, capturing 2005VL1 is the most attractive target, with the retrieved mass of the asteroid 292 and 390 times more than that of the spacecraft itself, corresponding to bi-impulse capture and single impulse asteroid capture strategies. Therefore, the asteroid 2005 VL1 can be considered to be the best candidate asteroid, whether minimizing the total Δv cost or maximizing the fraction of retrieved mass to the required spacecraft mass. In addition, the semi-major axis of this target asteroid is not close to the Earth's. This indicates that although only a small manoeuvre is required to move the asteroid from its initial orbit to the vicinity of the Earth, the relative velocity of the asteroid with respect to the Earth should be considerable and thus it would need a large impulse to insert it onto a stable manifold associated with a periodic orbit around the Sun-Earth libration points L_1/L_2. Therefore, this asteroid is not in the list of EROs [9].

Table 3 Results of bi-impulsive capture of asteroids to Earth orbit when optimizing f_m

Asteroid	Diameter, D	Capture date T_0, MJD	Flight time, day	Mass ratio f_m	Total cost, m/s	Mass loss f, %
1998 KY26	26.9	60364.2	111.4	51.1	39.3	15.6
2003 YS70	5.1	59779.5	146.5	95.6	20.6	18
2005 TH50	8.5	60584.7	1461	38.3	49	19.8
2005 VL1	13.5	59371.8	143.9	292.2	5.7	31
2007 UD6	7.4	63206.1	678	109.3	15.5	29.5
2008 EK68	4.1	60608.7	497	162.5	6.7	59.6
2008 UA202	4.5	60878.5	1545.5	58.7	38	4.9
2008 WM61	15.5	59874.1	1490.3	46.2	36.7	27.9
2009 WD54	6.8	61057.8	1401.6	172.6	8.7	39.6
2010 TW54	10.2	60054.1	1262.4	35.1	38	44.2
2010 UY7	6.8	60118.1	1585	62.7	32.9	11.7
2010 VO21	6.2	63809.9	1186.6	59.2	31.6	22.5
2010 XT10	17	61917.7	191.5	35.7	50.4	34.8
2012 BV1	2.1	59595.7	363.5	113.5	9.9	53.7
2012 EP10	5.1	60808.6	294.1	111.1	18.7	12.6

2012 HG2	13.5	59653.3	1055.4	59.3	34.4	13.2
2012 VC26	6.2	59525.5	1460.7	36.8	44.8	29.4
2013 GM3	18.6	59713.3	1430.6	33.5	43.7	40.9
2014 GQ17	12.9	62016.8	212.4	34	48.9	36
2014 JR24	4.7	59118.5	1689.6	127.1	16.4	11.4
2014 QN266	18.6	59745.6	1730.7	71.1	30.7	7.3
2014 WE6	2.8	63497.9	1148.3	84.2	23.5	15.7
2015 PS228	5.5	62174.3	1614.5	44.3	49.2	8.4

Table 4 Results of single impulse capture of asteroids to Earth orbit when optimizing f_m

Asteroid	Diameter, D	Capture date T_0, MJD	Flight time, day	Mass ratio f_m	Total cost, m/s	Mass loss f, %
1998 KY26	26.9	60368.8	107.6	53.2	37.8	15
2003 YS70	5.1	59779.4	146.6	100.4	19.5	51.6
2005 TH50	8.5	60581	1464.8	39.4	47.5	40
2005 VL1	13.5	59374.9	140.7	389.8	4.2	31.8
2007 UD6	7.4	63219.6	664.4	96.5	17.2	30.5
2008 EK68	4.1	60604.3	501.4	218	4.5	68.8
2008 UA202	4.5	60859.7	1563.9	63.4	35.2	6
2008 WM61	15.5	59871.1	1493.9	54.3	31.2	29.3
2009 WD54	6.8	61072.8	1386.2	213.6	6.7	60.1
2010 TW54	10.2	60068.7	1248.1	41.7	31.6	46.1
2010 UY7	6.8	60107.9	1594.9	69.4	29.7	40.8
2010 VO21	6.2	63803.2	1193.3	73	25.5	46.5
2010 XT10	17	61914.3	194.5	48.8	35.8	38.8
2012 BV1	2.1	59595.6	363.5	143.6	7.6	58.9
2012 EP10	5.1	60808.1	294.5	115.6	17.9	31.8
2012 HG2	13.5	59669.6	1038.6	64.3	31.7	17
2012 VC26	6.2	59512.5	1474	41	40.1	35.8

2013 GM3	18.6	59692.9	1450.9	39.4	36.4	41.3
2014 GQ17	12.9	62034	195.2	37.2	43.5	31.1
2014 JR24	4.7	59089.4	1718.1	126.5	16.4	52.4
2014 QN266	18.6	59748.6	1727.8	83.2	26.2	15.3
2014 WE6	2.8	63498.1	1148.1	85	23.2	44.8
2015 PS228	5.5	62175.8	1613.3	42.8	50.9	47.9

6. Conclusions

Two strategies have been proposed for capturing near-Earth asteroids to Earth orbit by using a single-pass aerobraking manoeuvre. Although aerobraking can increase risk during capture manoeuvres due to the requirement for a grazing flyby, a selection criterion for candidate asteroids was investigated to minimise such risks. Then, single impulse and bi-impulse capture of asteroids was discussed, using the total impulse and the yield of the retrieved mass of the asteroid with respect to the required spacecraft mass as objective functions. The results of these two capture strategies using aerobraking show that both strategies can achieve low-energy capture of asteroids to orbits around the Earth. Optimisation then finds the best candidate asteroids which can captured using aerobraking. This indicates that 2005 VL1 is one of the best targets which can be captured with a total cost below 10 m/s. Moreover, considering mass loss during aerobraking, capturing 2005 VL1 is also the most economical and the retrieved mass can be over 200 times more than that of the spacecraft which is required to execute the mission.

The strategies proposed are intended to be used for the preliminary analysis of aerobraking for asteroid capture. For the practical implementation of this concept, a real ephemeris model must be taken into account, along with robust navigation and control. However, since the model of the Sun-Earth circular restricted three-body problem can provide a good approximation of the real Sun-Earth system, the list of the near-Earth asteroids that can be captured with low energy are not expected to change significantly.

Acknowledgments

We acknowledge support through the China Scholarship Council (Minghu Tan) and a Royal Society Wolfson Research Merit Award (Colin McInnes).

References

[1] J. Lieske, Galilean satellites and the Galileo space mission, Celest. Mech. Dyn. Astron, 66 (1997) 13-20.

[2] D.E. Brownlee, P. Tsou, J. Anderson, M. Hanner, R. Newburn, Z. Sekanina, B. Clark, F. Hörz, M. Zolensky, J. Kissel, Stardust: Comet and interstellar dust sample return mission, Journal of Geophysical Research: Planets, 108 (2003) 1-15.

[3] W.H. Blume, Deep impact mission design, Space Science Reviews, 117 (2005) 23-42.

[4] K.-H. Glassmeier, H. Boehnhardt, D. Koschny, E. Kührt, I. Richter, The Rosetta mission: flying towards the origin of the solar system, Space Science Reviews, 128 (2007) 1-21.

[5] M.J. Sonter, The technical and economic feasibility of mining the near-earth asteroids, Acta Astronaut., 41 (1997) 637-647.

[6] J. Sanchez, C. McInnes, Asteroid resource map for near Earth space, J. Spacecrat Rockets, 48 (2011) 153-165.

[7] J.P. Sanchez, D. Garcia Yarnoz, C. McInnes, Near-Earth asteroid resource accessibility and future capture mission opportunities, in: Global Space Exploration Conference. Paper GLEX-2012.11.1.5x12412, Washington, DC, 2012.

[8] Z. Hasnain, C.A. Lamb, S.D. Ross, Capturing near-Earth asteroids around Earth, Acta Astronaut., 81 (2012) 523-531.

[9] D.G. Yárnoz, J. Sanchez, C. McInnes, Easily retrievable objects among the NEO population, Celest. Mech. Dyn. Astron, 116 (2013) 367-388.

[10] G. Tang, F. Jiang, Capture of near-Earth objects with low-thrust propulsion and invariant manifolds, Astrophys. Space Sci., 361 (2016) 1-14.

[11] G. Mingotti, J. Sánchez, C. McInnes, Combined low-thrust propulsion and invariant manifold trajectories to capture NEOs in the Sun–Earth circular restricted three-body problem, Celest. Mech. Dyn. Astron, 120 (2014) 309-336.

[12] J.P. Sánchez, D.G. Yárnoz, Asteroid retrieval missions enabled by invariant manifold dynamics, Acta Astronaut., 127 (2016) 667-677.

[13] J.R. Brophy, L. Friedman, F. Culick, Asteroid retrieval feasibility, in, Keck Institute for Space Studies, California Institute of Technology, Jet Propulsion Laboratory, Pasadena, California, 2012.

[14] G. Mingotti, J.-P. Sanchez, C. McInnes, Low energy, low-thrust capture of near Earth objects in the Sun–Earth and Earth–Moon restricted three-body systems, in: SPACE Conferences & Exposition, AIAA 2014-4301, AIAA, Washington, 2014.

[15] M. Tan, C. McInnes, M. Ceriotti, Direct and indirect capture of near-Earth asteroids in the Earth–Moon system, Celest. Mech. Dyn. Astron, 129 (2017) 57-88.

[16] S. Gong, J. Li, Asteroid capture using lunar flyby, Adv. Space Res., 56 (2015) 848-858.

[17] P.E. Verrier, C.R. McInnes, Low-Energy Capture of Asteroids onto Kolmogorov–Arnold–Moser Tori, J. Guid. Contr. Dynam., 38 (2014) 330-335.

[18] R.W. Farquhar, D.W. Dunham, Y. Guo, J.V. McAdams, Utilization of libration points for human exploration in the Sun–Earth–Moon system and beyond, Acta Astronaut., 55 (2004) 687-700.

[19] N. Lladó, Y. Ren, J.J. Masdemont, G. Gómez, Capturing small asteroids into a Sun–Earth Lagrangian point, Acta Astronaut., 95 (2014) 176-188.

[20] J.P. Sanchez, C.R. McInnes, On the ballistic capture of asteroids for resource utilisation, in: 62nd International Astronautical Congress, IAC-11.C1.4.6, CapeTown, SA, 2011.

[21] M. Tan, C.R. McInnes, M. Ceriotti, Low-Energy Near-Earth Asteroid Capture Using Momentum Exchange Strategies, J. Guid. Contr. Dynam., 41 (2017) 632-643.

[22] D. Carrelli, D. O'Shaughnessy, T. Strikwerda, J. Kaidy, J. Prince, R. Powell, Autonomous aerobraking for low-cost interplanetary missions, Acta Astronaut., 93 (2014) 467-474.

[23] Z.R. Putnam, R.D. Braun, Drag-modulation flight-control system options for planetary aerocapture, J. Spacecrat Rockets, 51 (2013) 139-150.

[24] D.A. Spencer, R. Tolson, Aerobraking cost and risk decisions, J. Spacecrat Rockets, 44 (2007) 1285-1293.

[25] R.Y. Jits, G.D. Walberg, Blended control, predictor–corrector guidance algorithm: an enabling technology for Mars aerocapture, Acta Astronaut., 54 (2004) 385-398.

[26] D.T. Lyons, W. Sjogren, W.T. Johnson, D. Schmitt, A. McRonald, Aerobraking Magellan, in: Astrodynamics 1991, San Diego, CA, 1992, pp. 1821-1839.

[27] D.T. Lyons, J.G. Beerer, P. Esposito, M.D. Johnston, W.H. Willcockson, Mars global surveyor: aerobraking mission overview, J. Spacecrat Rockets, 36 (1999) 307-313.

[28] R.D. Braun, R.W. Powell, J. Lyne, Earth aerobraking strategies for manned return from mars, J. Spacecrat Rockets, 29 (1992) 297-304.

[29] M. Kumar, A. Tewari, Trajectory and attitude simulation for aerocapture and aerobraking, J. Spacecrat Rockets, 42 (2005) 684-693.

[30] H.X. Baoyin, Y. Chen, J.F. Li, Capturing near earth objects, Research in Astronomy and Astrophysics, 10 (2010) 587.

[31] T. Heppenheimer, Approximate analytic modeling of a ballistic aerobraking planetary capture, J. Spacecrat Rockets, 8 (1971) 554-555.

[32] J.P. Sanchez, C. McInnes, Synergistic approach of asteroid exploitation and planetary protection, Adv. Space Res., 49 (2012) 667-685.

[33] L. Fast, Capture a 2m Diameter Asteroid, a Mission Proposal, in: AIAA SPACE 2011 Conference & Exposition, AIAA 2011-7116 AIAA, Long Beach, California, 2011, pp. 1-10.

[34] M. Tan, C. McInnes, M. Ceriotti, Low-energy near Earth asteroid capture using Earth flybys and aerobraking, Adv. Space Res., 61 (2018) 2099-2115.

[35] S.D. Ross, Near-earth asteroid mining, in: Space, Department of Control and Dynamical Systems, Pasadena, CA, , 2001, pp. 1-24.

[36] E. Kolemen, N.J. Kasdin, P. Gurfil, Multiple Poincaré sections method for finding the quasiperiodic orbits of the restricted three body problem, Celest. Mech. Dyn. Astron, 112 (2012) 47-74.

[37] V. Szebehely, Theory of orbit: The restricted problem of three Bodies, Academic Press, New York, 1967.

[38] W.S. Koon, M.W. Lo, J.E. Marsden, S.D. Ross, Dynamical systems, the three-body problem and space mission design, Springer-Verlag, New York, 2011.

[39] D.A. Vallado, Fundamentals of astrodynamics and applications, Springer, New York, 2007.

[40] S.R. Chesley, P.W. Chodas, A. Milani, G.B. Valsecchi, D.K. Yeomans, Quantifying the risk posed by potential Earth impacts, Icarus, 159 (2002) 423-432.

[41] S. Love, D. Brownlee, Heating and thermal transformation of micrometeoroids entering the Earth's atmosphere, Icarus, 89 (1991) 26-43.

[42] V. Svetsov, I. Nemtchinov, A. Teterev, Disintegration of large meteoroids in Earth's atmosphere: Theoretical models, Icarus, 116 (1995) 131-153.

[43] H. Atkinson, C. Tickell, D. Williams, Report of the task force on potentially hazardous near Earth objects, in, British National Space Centre, London, , 2000.

[44] T. Gehrels, M.S. Matthews, A. Schumann, Hazards due to Comets and Asteroids, University of Arizona Press, Tucson, Arizona, 1994.

[45] M. Vasile, C. Colombo, Optimal impact strategies for asteroid deflection, J. Guid. Contr. Dynam., 31 (2008) 858-872.

[46] C. Gritzner, K. Dürfeld, J. Kasper, S. Fasoulas, The asteroid and comet impact hazard: risk assessment and mitigation options, Naturwissenschaften, 93 (2006) 361-373.

[47] A. Harris, M. Boslough, C. Chapman, L. Drube, P. Michel, A. Harris, Asteroid Impacts and Modern Civilization: Can We Prevent a Catastrophe?, in: P. Michel, F.E. DeMeo, W.F. Bottke (Eds.) Asteroids IV, University of Arizona Press, Arizona, 2015, pp. 835-854.

[48] B. Tauzin, E. Debayle, C. Quantin, N. Coltice, Seismoacoustic coupling induced by the breakup of the 15 February 2013 Chelyabinsk meteor, Geophysical Research Letters, 40 (2013) 3522-3526.

[49] J.W. Birks, P.J. Crutzen, R.G. Roble, Frequent ozone depletion resulting from impacts of asteroids and comets, in: P. Bobrowsky, H. Rickman (Eds.) Comet/Asteroid Impacts and Human Society: An Interdisciplinary Approach, Springer, Berlin, 2007, pp. 225-245.

[50] E. Belbruno, Capture dynamics and chaotic motions in celestial mechanics: With applications to the construction of low energy transfers, Princeton University Press, 2004.

[51] G. Cook, Luni-solar perturbations of the orbit of an earth satellite, Geophysical Journal International, 6 (1962) 271-291.

[52] M. Ceriotti, Global optimisation of multiple gravity assist trajectories, in, University of Glasgow, 2010.

[53] E.W. Weisstein, Sphere point picking, in, 2002.

[54] K. Deb, A. Pratap, S. Agarwal, T. Meyarivan, A fast and elitist multiobjective genetic algorithm: NSGA-II, IEEE Trans. Evol., 6 (2002) 182-197.